Int. J. Heat Mass Transfer. Vol. 21, pp. 269–274. Pergamon Press 1978. Printed in Great Britain

THERMAL INTERACTIONS AMONG THE CONFINING WALLS OF A TURBULENT RECIRCULATING FLOW

S. V. PATANKAR, E. M. SPARROW and M. IVANOVIĆ
Department of Mechanical Engineering, University of Minnesota, Minneapolis, MN 55455, U.S.A.

(*Received* 24 *February* 1977 *and in revised form* 10 *June* 1977)

Abstract—Numerical solutions for the velocity and temperature fields in a cylindrical enclosure have been obtained to determine how the heat transfer at any one of the bounding walls is affected by the thermal boundary conditions at the other walls. The enclosure is a hollow cylinder closed at both ends by circular disks. A recirculating flow is induced within the enclosure by a fluid throughflow which enters via a central aperture in one of the disks and exits via an annular gap at the rim of the other disk. The analysis is based on the k-ε turbulence model, and the solutions were carried out by an elliptic finite difference procedure. Results were obtained for parametric values of the Reynolds number of the entering throughflow and of the length-to-radius ratio of the enclosure. The results show that the heat-transfer rates at the outlet disk and at the cylindrical wall are not greatly affected by the thermal boundary conditions at the other surfaces. On the other hand, the heat-transfer rate at the inlet disk is more sensitive to the thermal conditions at the other surfaces.

NOMENCLATURE

- A, area of a surface;
- h, local heat-transfer coefficient, $q/(T_w - T_i)$;
- h^*, average heat-transfer coefficient for solo heating conditions, $Q^*/A(T_w - T_i)$;
- k, thermal conductivity;
- k, turbulence kinetic energy;
- L, spacing between disks;
- Pr, Prandtl number;
- Pr_t, turbulent Prandtl number;
- Q, rate of heat transfer at a given surface;
- Q^*, rate of heat transfer for solo heating conditions;
- q, local heat flux;
- $\bar{q}$, average heat flux for a given surface;
- R, radius of enclosure;
- Re, pipe Reynolds number of flow through inlet aperture;
- r, radial coordinate;
- T_i, inlet temperature;
- T_w, wall temperature;
- X, axial coordinate;
- ε, dissipation rate of turbulence kinetic energy.

Subscripts

- DI, inlet disk;
- DO, outlet disk;
- S, cylindrical shroud.

INTRODUCTION

IN FLOWS where there is a principal direction of fluid motion, thermal processes at upstream surfaces are generally unaffected by the heat transfer taking place at downstream surfaces. On the other hand, in the presence of recirculating flows, there may be strong thermal interactions among all the surfaces which bound the flow. Recirculating flows are frequently encountered in partially or fully enclosed spaces which are bounded by surfaces having different and autonomous thermal boundary conditions. It is, therefore, of practical interest to investigate how the heat transfer at a given surface of an enclosure is affected by changes in the thermal boundary conditions at the other surfaces. Such an investigation is the subject of this paper.

The flow situation to be analyzed here is portrayed schematically in Fig. 1, which shows a cylindrical enclosure with fluid throughflow. Fluid enters the enclosure through a central aperture in one of the disks and exits via an annular gap at the rim of the other disk. As indicated by the streamlines sketched in the figure, the enclosure is filled with a large recirculation zone. The disk which houses the fluid inlet aperture will be denoted by DI, that which houses the fluid outlet by DO, and the cylindrical shroud by S.

The enclosure and throughflow arrangement pictured in Fig. 1 is the same as that employed in the

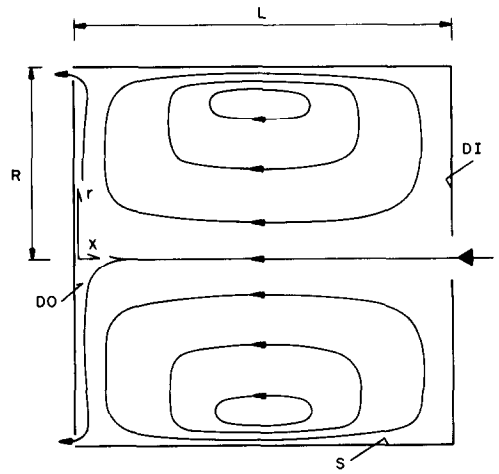

FIG. 1. Schematic of the enclosure.

experiments of [1]. In those experiments, the cylindrical shroud was heated while both the inlet and outlet disks were unheated. The reported Nusselt numbers for the shroud are, strictly speaking, applicable only to those cases which correspond to the boundary conditions of the experiments. The sensitivity of these Nusselt number results to other boundary conditions, for instance, to heating of either one or both of the disks, is not known. This situation well illustrates and motivates the aim of the present research to investigate the thermal response of each surface of the enclosure to the boundary conditions at the other surfaces.

The approach to be employed in this study will now be outlined. Attention is first focused on one of the surfaces, for instance, the shroud, and a succession of four cases are considered and the corresponding solutions carried out by a numerical finite difference procedure. In the first case, the shroud is heated while both disks are adiabatic. The second case is characterized by heating at the shroud and the inlet disk, with the outlet disk adiabatic. For the third case, the shroud and the outlet disk are heated, and the inlet disk is adiabatic. All three surfaces are heated in the fourth case. For each case, the heated surfaces are maintained at the same uniform temperature. This approach is employed successively for the shroud and for each of the disks as the primary focus of attention.

For fixed values of the geometrical and flow parameters, the highest rate of heat transfer at a given surface occurs when only that surface is heated and the others are adiabatic. Thus, the solo-heated case for a given surface is taken as a standard for assessing the reduction in heat transfer at that surface when there is heating at the other walls of the enclosure. In accordance with this, the principal heat transfer results are presented in ratio form relative to the solo-heated case.

The analysis was performed for turbulent flow in the enclosure. Results were obtained for parametric values of the inlet Reynolds number Re and of the spacing-to-radius ratio L/R, respectively ranging from 15 000 to 47 000 and from 0.44 to 2. The choice of these ranges was influenced by the experiments of [1], as was the value of 0.7 for the Prandtl number (air). The radius of the outlet disk (0.944R) and of the aperture of the inlet disk (0.11R) were also motivated by the apparatus of [1].

ANALYSIS

The analysis is based on the k-ε turbulence model as outlined in [2] and the finite difference procedure of [3], and only a brief discussion of the adaptation of these methods is appropriate. The k-ε model has yielded satisfactory predictions in a variety of turbulent flow situations but has not been extensively used in the study of recirculating flows. Therefore, to provide further perspective about its capabilities with regard to recirculating flows, comparisons between the predictions of the k-ε model and the experimental results of [1] will be made later in the paper.

The main differential equations to be solved are the time-averaged conservation equations for mass, momentum, and energy. The turbulent stresses and the turbulent heat fluxes in these equations are expressed via a turbulent viscosity and a turbulent Prandtl number. The local turbulent viscosity is assumed to depend on the turbulence kinetic energy k and its dissipation rate ε. Two additional differential equations are formulated for k and ε, which are to be solved simultaneously with the above-mentioned conservation equations. The values of the numerical constants which appear in the k-ε turbulence model were taken directly from Table 2.1 of [2] and were not adjusted to force agreement between the analytical predictions and the experimental data of [1]. The constants tabulated in [2] had been deduced from comparisons between analysis and experiments for flow configurations that are quite different from that considered here.

In the present work, the k-ε model is used throughout the entire enclosure except in a narrow region adjacent to the walls. This region is treated by the wall-function method. In the version of this method described in [2], it is assumed that at the outer boundary of the region, the velocity and temperature profiles obey the "universal" logarithmic law of the wall. Since it is known that the logarithmic law is valid for values of y^+ greater than about 15 ($y^+ = y(\tau_w/\rho)^{1/2}/\nu$ is the "universal" wall distance coordinate), the wall-adjacent nodes in the finite difference grid were positioned so that their y values satisfied this constraint. In particular, with all wall-adjacent nodes having a common value of y along a given wall and with $(\tau_w/\rho)^{1/2}$ varying along the wall, the corresponding y^+ values also vary. The constraint that $y^+ \geqslant \sim 15$ was imposed at the wall-adjacent node having the smallest value of y^+, so that substantially larger y^+ values ($\sim$ 50–100) existed at other wall-adjacent nodes. The value of the von Karman constant which appears in the law of the wall was evaluated in accordance with equation (11) of [4] using the constants from Table 2.1 of [2].

The solution of the energy equation requires that the turbulent Prandtl number Pr_t be specified. For simple boundary layer and pipe flows, it has been found that $Pr_t = 0.9$ gives predictions that are in satisfactory agreement with experiment. On the other hand, jets and mixing layers require a value as low as 0.5 ([5], p. 661 and [6]). For a complex situation such as the one considered here, there is considerable uncertainty about the proper value of Pr_t. On the basis of a comparison with experiment to be presented later, the value of $Pr_t = 0.5$ was chosen because it yielded Nusselt number predictions that agreed better with the data than did those for $Pr_t = 0.9$.

The k-ε turbulence model requires that numerical values of k and ε be given at the inlet cross section, i.e. at the aperture of the inlet disk. If it is assumed that the flow passing through the aperture is a standard fully developed turbulent pipe flow, then k values between 0.5 and 1.5% of the mean kinetic energy are typical [7]. The corresponding values of ε were deduced from equation (2.1–2) of [2] by assuming a representative mixing length to be in the range 1/20 to 1/10 of the radius of the inlet pipe ([5], p. 568). Computational

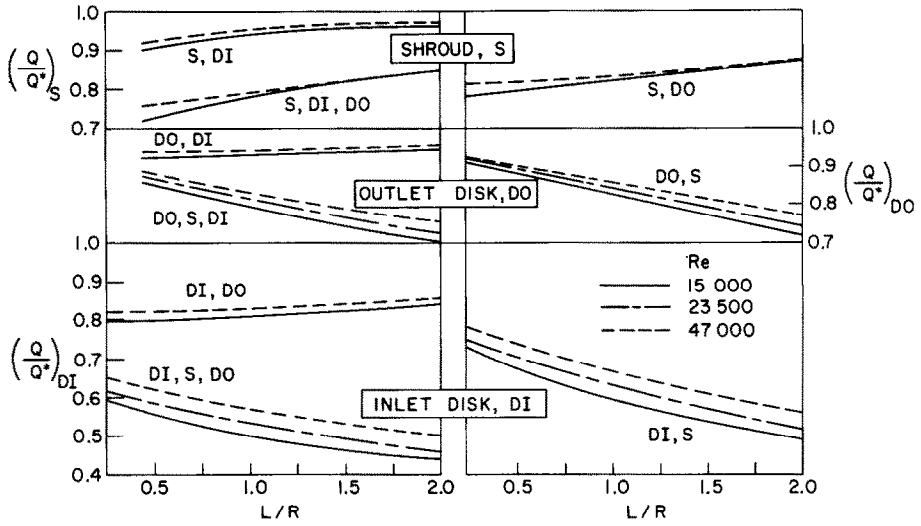

FIG. 2. Response of the heat transfer at a given surface to the thermal boundary conditions at the other surfaces.

experiments demonstrated that the results were altogether insensitive to variations of the inlet values of k and ε in these ranges.

The governing equations were formulated for constant thermophysical properties and axisymmetric flow and heat transfer. They form a set of six two-dimensional elliptic partial differential equations, which are solved by a finite difference procedure. The governing equations are elliptic because the axial and radial diffusion terms have been retained for both momentum and energy and, in addition, the pressure field is unknown. The elliptic system requires that closure conditions be given at the downstream end of the solution domain. In the present problem, it was assumed that all x-derivatives are zero at the exit aperture.

The finite difference method used here is a straightforward adaptation of that of [3]. In [3], a procedure is described for three-dimensional parabolic flows which involves marching in the main flow direction while solving a two-dimensional elliptic problem at each marching station. Thus, there is imbedded in [3] a finite difference scheme for dealing with two-dimensional elliptic problems. That scheme was extracted and employed in the present problem.

The finite difference grid was laid out with 16 nodal points along the radial coordinate and 20 nodal points along the axial coordinate. The points were deployed with a somewhat higher density adjacent to the walls of the enclosure. The coordinates of the nodal points are as follows:

$x/L = 0, 0.011, 0.039, 0.078, 0.128, 0.183, 0.239, 0.300, 0.367, 0.439, 0.517, 0.589, 0.656, 0.717, 0.772, 0.828, 0.883, 0.933, 0.978, 1.0$

$r/R = 0, 0.011, 0.039, 0.083, 0.150, 0.233, 0.322, 0.417, 0.522, 0.628, 0.728, 0.822, 0.905, *, *, 1.0$

The points denoted by asterisks were adjusted from case to case in order to fulfill the y^+ constraint that was discussed earlier.

RESULTS

The response of the heat transfer at each surface of the enclosure to the thermal boundary conditions at the other surfaces is exhibited in Fig. 2. The figure is subdivided into three parts that are arranged one above the other. From top to bottom, the respective parts contain heat-transfer results for the shroud, the outlet disk, and the inlet disk.

The ordinate variable for each part is a ratio of heat transfer rates at the surface in question. The denominator Q^* corresponds to the case where that surface alone is heated, whereas the numerator Q is for the case where one or both of the other surfaces are also heated (all at the same uniform temperature). The curves are labelled to identify the heating conditions. Thus, for example, the designation S, DI indicates that both the shroud and the inlet disk are heated. In addition, the Reynolds number of the flow passing through the inlet aperture is identified by solid, dashed, or dot-dashed lines. The abscissa is the ratio of the separation distance L between the disks to the radius R.

Inspection of the figure indicates that, as expected, the rate of heat transfer at a given surface is diminished when the other surfaces of the enclosure are heated. However, neither the shroud nor the outlet disk are greatly affected by the presence of heating at the other surfaces, as witnessed by the fact that $Q/Q^* > 0.7$ for all curves in the upper and middle portions of the figure. Thus, any available heat-transfer coefficients for the shroud and for the outlet disk can be accorded a rather broad range of applicability with respect to thermal boundary conditions at the other surfaces of the enclosure. On the other hand, the inlet disk is more affected by the other surfaces, as evidenced by Q/Q^* values as low as 0.44 in the lower part of the figure. Therefore, heat-transfer coefficients for the inlet disk which correspond to specific thermal boundary conditions do not apply with high accuracy for other boundary conditions.

The trends of the Q/Q^* results with the enclosure aspect ratio L/R are physically plausible. As the length L of the shroud increases, it becomes less sensitive to the thermal boundary conditions at the other surfaces. In contrast, both the inlet and outlet disks become more responsive to the shroud at larger values of L, but they are less affected by each other.

Average Nusselt numbers for solo heating of the respective surfaces are listed in Table 1. The heat-transfer coefficient h^* was evaluated as $Q^*/A(T_w - T_i)$, where A is the area of the respective surface and T_w and T_i are, respectively, the wall temperature and inlet fluid temperature.

Table 1. Average heat-transfer coefficients

L/R	Re	$(h^*L/k)_s$	$(h^*R/k)_{DO}$	$(h^*R/k)_{DI}$
0.44	15 000	60.0	201.2	79.4
	23 500	92.9	307.0	113.9
	47 000	151.7	571.3	213.4
0.89	15 000	86.0	212.2	78.7
	23 500	122.4	327.2	122.5
	47 000	219.9	614.7	232.4
2.0	15 000	113.5	185.8	43.8
	23 500	168.4	284.6	64.2
	47 000	298.4	529.2	112.6

The results presented in Fig. 2 and Table 1 pertain to the heat-transfer performance of each surface as a whole. Representative results for the local heat flux distributions on the respective surfaces will now be presented, and Fig. 3 has been prepared for this purpose. In this figure, the ordinate variable $q/\bar{q}$ is the ratio of the local heat flux to the average heat flux, with the average being specific to each surface. The left-hand and right-hand panels of the figure respectively convey results for the disks and for the shroud. Since $\bar{q}$ is a radius-weighted average of q for each disk, the areas under the curves in the left-hand panel are not equal to unity.

For each surface, local heat flux distributions were available for four cases encompassing various heating conditions at the other surfaces of the enclosure. However, for the most part, these distributions were so overlapped that they could not be plotted as separate curves in the figure. For the shroud and the inlet disk, the overall spread among the available results is indicated. A somewhat more distinct separation among the results is in evidence for the outlet disk. The results of Fig. 3 are for the intermediate parameter values $L/R = 0.89$ and $Re = 23\,500$, but the trends are applicable for all of the cases investigated here.

Inspection of Fig. 3 indicates that the local heat flux on the shroud decreases monotonically along the direction of the recirculating flow which washes the shroud surface. The heat flux on the inlet disk also decreases along the recirculating flow direction, but there is a sharp rise adjacent to the aperture where the recirculation interacts with the incoming throughflow stream. For the outlet disk, the highest values of the heat flux occur in the region where the throughflow stream impinges on the disk surface. Subsequently, the impinged fluid forms a wall jet which grows thicker as it flows radially outward along the disk, with a consequent decrease in the local heat flux.

To provide an indication of the effectiveness of the k-ε turbulence model in coping with the complexities of the flow and temperature field, solutions have been carried out to facilitate comparisons with the experiments of [1]. In those experiments, only the shroud was heated. The heating was accomplished by electrical resistance tape wrapped around the convex surface of the stainless steel cylindrical sheet that formed the shroud. In the processing of the experimental data, it was assumed that a uniform heat flux was supplied to the shroud. The convective heat flux to the fluid was evaluated by taking account of axial conduction in the stainless steel sheet, the magnitude of the conduction being determined from the measured wall temperatures.

For the numerical solutions that were performed for comparison with the experiments, the actual wall

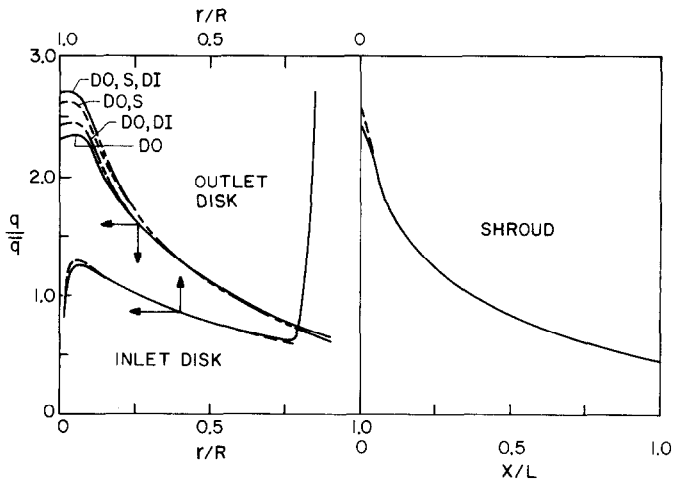

FIG. 3. Representative local heat flux distributions, $L/R = 0.89$ and $Re = 23\,500$.

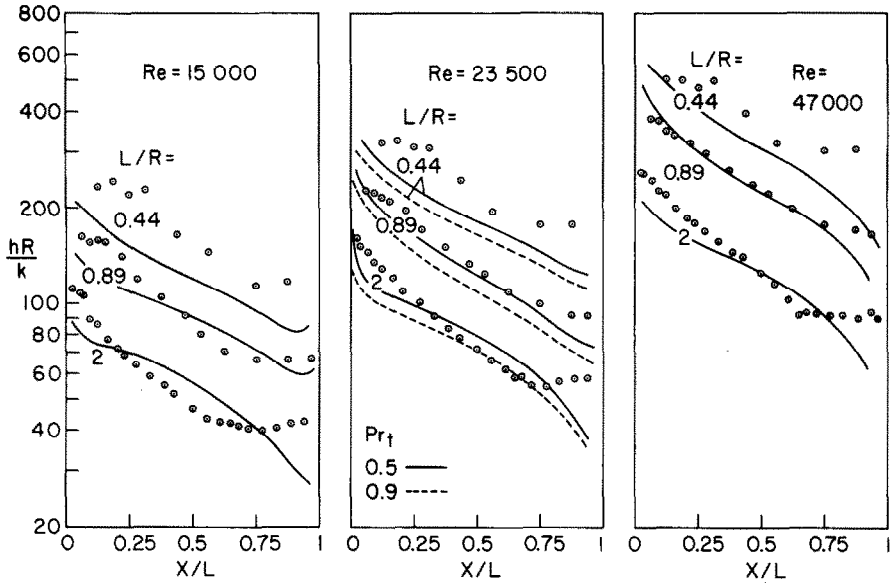

FIG. 4. Comparison of predicted local heat-transfer coefficients for the cylindrical shroud with the experimental values of [1].

temperature data from the experiments were employed as input to the computer program. With the local heat flux results provided by the solutions, local heat transfer coefficients were evaluated from the relation $h = q/(T_w - T_i)$.

A comparison of the predicted local heat-transfer coefficients for the shroud with those of experiment [1] is presented in Fig. 4. The figure is subdivided into three panels, each of which pertains to a specific Reynolds number. In each panel, results are given for the three aspect ratios that were investigated. In the main, the analytical predictions correspond to a turbulent Prandtl number Pr_t of 0.5 (solid lines). To illustrate the sensitivity of the results to Pr_t, predictions corresponding to $Pr_t = 0.9$ are also shown in the middle panel (dashed lines).

From the figure, it is seen that there is generally satisfactory agreement between the experimental results and the analytical predictions for $Pr_t = 0.5$. Although some data points lie above the predictions and others lie below, there is a general tendency for the data to fall on the high side. In view of the complexity of the flow and the expected accuracy of the experiments, the level of agreement in evidence in the figure is supportive of the analytical model and, therefore, of the results of Figs. 2 and 3.

In some cases, there appears to be a lower level of agreement near the respective ends of the shroud. This may well be due to imperfections of the guard heating in the experiments and to the relatively large corrections for axial conduction which involved numerical second derivatives of the measured wall temperatures. These effects are accentuated at smaller aspect ratios (i.e. shorter shroud lengths), and this may account for the somewhat larger deviations between analysis and experiment at smaller L/R.

The use of $Pr_t = 0.9$ in the calculations is seen to bring about larger, but not wholly unacceptable, deviations between the predictions and the data. In the opinion of the authors, the superior level of agreement afforded by $Pr_t = 0.5$ warranted its use in the solutions that led to Figs. 2 and 3.

As a final matter, mention may be made of an interesting characteristic of the fluid flow solutions. For all of the nine cases studied here, the mass flow rate of the recirculating fluid was compared with the mass flow rate of the throughflow. In all cases, the two flow rates were found to be essentially equal, with the greatest deviation being about 25%.

Acknowledgement—This research was performed under the auspices of NSF Grant ENG-7518141.

REFERENCES

1. E. M. Sparrow and L. Goldstein, Jr., Effect of rotation and coolant throughflow on the heat transfer and temperature field in an enclosure, *J. Heat Transfer* **98**, 387–394 (1976).
2. B. E. Launder and D. B. Spalding, The numerical computation of turbulent flows, *Comput. Meth. Appl. Mech. Engng* **3**, 269–289 (1974).
3. S. V. Patankar and D. B. Spalding, A calculation procedure for heat, mass and momentum transfer in three-dimensional parabolic flows, *Int. J. Heat Mass Transfer* **15**, 1787–1806 (1972).
4. P. L. Stephenson, A theoretical study of heat transfer in two-dimensional turbulent flow in a circular pipe and between parallel and diverging plates, *Int. J. Heat Mass Transfer* **19**, 413–423 (1976).
5. H. Schlichting, *Boundary Layer Theory*, 6th edn. McGraw-Hill, New York (1968).
6. G. N. Abramovitch, *The Theory of Turbulent Jets*. MIT Press, Cambridge, MA (1963).
7. J. Laufer, The structure of turbulence in fully developed pipe flow, NACA Report 1174 (1969).

INTERACTIONS THERMIQUES ENTRE PAROIS QUI DELIMITENT UN ECOULEMENT TURBULENT AVEC RECIRCULATION

Résumé—On obtient les solutions numériques des champs de vitasse et de température dans une enceinte cylindrique pour déterminer comment le transfert thermique à une paroi quelconque est modifié par les conditions thermiques sur les autres parois. La cavité est un cylindre fermé aux deux extrémités par des disques. Un écoulement de recirculation est induit par une fente annulaire sur le pourtour de l'autre disque. L'analyse est basée sur le modèle $k-\varepsilon$ de turbulence et les solutions sont cherchées par une procédure aux différences finies. Des résultats sont obtenus pour des valeurs paramétriques du nombre de Reynolds à l'entrée et du rapport longueur sur rayon de l'ouverture. Ils montrent que les flux thermiques au disque de sortie et à la paroi cylindrique ne sont pas fortement affectés par les conditions thermiques sur les autres surfaces. Par contre, le transfert thermique sur le disque d'entrée est plus sensible aux conditions thermiques sur les autres surfaces.

WÄRMEAUSTAUSCH AN GRENZFLÄCHEN FÜR EINE TURBULENTE REZIRKULIERENDE STRÖMUNG

Zusammenfassung—Numerische Berechnungen für die Geschwindigkeits- und Temperaturfelder in einem zylindrischen Behälter wurden durchgeführt, um die Beeinflussung der Wärmeübertragung an jeder einzelnen begrenzenden Wand, durch die thermischen Randbedingungen der anderen Wände zu untersuchen. Der Behälter ist ein hohler Zylinder, der an beiden Enden durch kreisförmige Scheiben geschlossen wird. Innerhalb des Behälters wird eine rezirkulierende Strömung so erzeugt, daß das Fluid in eine zentrale Oeffnung der einen Scheibe eintritt und durch eine ringförmige Oeffnung am Rande der anderen Scheibe austritt. Die Berechnung erfolgte nach dem k-ε-Turbulenzmodellund die Lösungen wurden mit einem elliptischen finiten Differenzenverfahren durchgeführt. Es wurden Ergebnisse für die Parameterwerte Reynoldzahl der Strömung am Eintritt sowie des Länge/Radius-Verhältnisses des Behälters erzielt. Die Ergebnisse zeigen, daß die Wärmestromdichte an der Austrittsscheibe und an der zylindrischen Wand nicht sonderlich durch die thermischen Randbedingungen an den anderen Oberflächen beeinflßt wird. Andererseits ist die Wärmestromdichte an der Eintrittsscheibe den thermischen Randbedingungen an den anderen Oberflächen gegenüber empfindlicher.

ТЕПЛОВЫЕ ВЗАИМОДЕЙСТВИЯ МЕЖДУ ОГРАНИЧИВАЮЩИМИ СТЕНКАМИ В ТУРБУЛЕНТНОМ РЕЦИРКУЛИРУЮЩЕМ ПОТОКЕ

Аннотация — Получены численные решения для полей скорости и температуры в цилиндрической замкнутой полости для определения влияния тепловых граничных условий на стенках на теплообмен на любой из ограничивающих стенок. Полость представляет собой полый цилиндр, закрытый с обоих концов круглыми дисками. Рециркулирующий поток индукцируется в цилиндре сквозным потоком жидкости, которая поступает через центральное отверстие в одном из дисков и выходит через кольцевой зазор другого диска. Анализ основан на использовании модели турбулентности $k-\varepsilon$, а решения найдены с помощью эллиптического конечно-разностного метода. Результаты получены для различных значений числа Рейнольдса для поступающего сквозного потока и отношения длины к радиусу цилиндра. Полученные результаты показывают, что тепловые граничные условия на других поверхностях не оказывают сильного влияния на скорости теплообмена вблизи выходного диска и на стенке цилиндра. С другой стороны, скорость теплообмена вблизи входного диска более чувствительна к тепловым условиям на других поверхностях.